Neutron-proton multiplets in odd-odd $^{106-116}$In nuclei

J. Van Maldeghem* and K. Heyde†
Institute for Nuclear Physics, B-9000 Gent, Belgium

J. Sau
Institut de Physique Nucléaire et IN2P3, 69622 Villeurbanne Cedex, France
(Received 1 April 1985)

A systematic study of neutron-proton multiplets in $^{106-116}$In isotopes is presented. Energy levels, wave functions, and magnetic dipole and electric quadrupole moments are calculated within the framework of neutron-quasiparticle proton-hole multiplets coupled to quadrupole phonon excitations of the underlying core. The role played by the neutron-proton interaction and the collective quadrupole vibrations is discussed.

I. INTRODUCTION

In the last few years, the amount of information on odd-odd nuclei in the $Z=50$ region has been extended considerably. With the help of heavy-ion reactions, the existence of collective bands was established. The study of such bands confirms our knowledge of collective behavior as deduced from the study of even-even and odd-even nuclei in the same region. In addition, it also enables us to draw conclusions about the residual neutron-proton interaction.

In the $^{106-116}$In nuclei, a negative parity band starting at $J^\pi=7^-$ (8^-) has been observed. This band can be assigned to the neutron quasiparticle-proton hole $1h_{11/2}$-$1g_{9/2}^{-1}$ multiplet. As the neutron number increases, the negative parity band head lowers in excitation energy and the band spacings become compressed. The latter can be seen from the fact that the energy difference between the 10^- state and the 7^- (8^-) band head decreases. Several approaches have been applied in order to understand the nature of these bands and/or the role played by the neutron-proton interaction: shell model,[1–3] quasiparticle model,[4–6] and rotor-plus-two-quasiparticle model.[7–10]

In this paper, we start from neutron-quasiparticle proton-hole multiplets coupled to a quadrupole vibrational core. This vibrational approach has already proven to be successful in the odd-A In isotopes[11–15] and in the odd-odd Sb region.[16–18]

The present calculation differs from the approaches mentioned in the previous paragraph in the following ways. First of all, a systematic study for a number of odd-odd In isotopes is presented. This is made possible because we presently dispose over a large amount of experimental data. Secondly, the combined effect of both the neutron-proton interaction and the collective excitations on the splitting of the $1h_{11/2}(\nu)$-$1g_{9/2}^{-1}(\pi)$ multiplet is included in the present model. Finally the influence of collective excitations in reproducing some experimental known magnetic and quadrupole moments of ground and first excited states is given.[19–31]

II. MODEL DESCRIPTION

A. Hamiltonian

The general form of the Hamiltonian can be written as

$$H=H_{\rm coll}+H_{\rm qp}(\nu)+H_{\rm sh}(\pi)+H_{\rm coupl}(\nu)+H_{\rm coupl}(\pi)+H_{\rm int}(\nu,\pi)\ , \tag{2.1}$$

where

$$H_{\rm coll}=\hbar\omega_2\sum_\mu b_{2\mu}^\dagger b_{2\mu}$$

describes the excitation energy of the underlying vibrational core ($b_{2\mu}^\dagger$ denotes the quadrupole phonon creation operator, $\hbar\omega_2$ the quadrupole phonon energy), and

$$H_{\rm qp}(\nu)=\sum_\nu E(\nu)N(c_\nu^\dagger c_\nu)$$

describes the unperturbed quasiparticle energy of the neutron [$E(\nu)$ denotes the neutron-quasiparticle energy, $c_\nu^\dagger$ the neutron-quasiparticle operator, and $N(\cdots)$ indicates

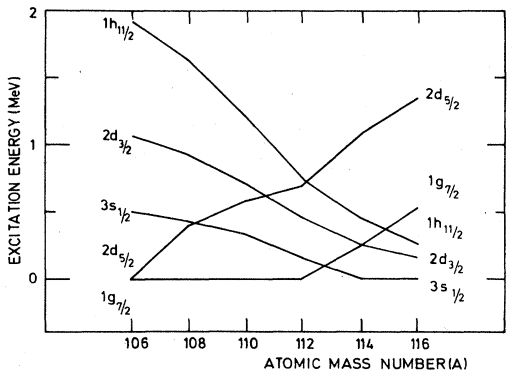

FIG. 1. Neutron-quasiparticle energies as used in the calculations of neutron-proton multiplets in the odd-odd $^{106-116}$In isotopes.

TABLE I. The proton single-hole energies $\tilde{\epsilon}_{nlj}(\pi)$ (in MeV, relative to the $1g_{9/2}^{-1}$ orbital) and the neutron one-quasiparticle energies $E_{nlj}(\nu)$ (in MeV) as used in the neutron-proton multiplet calculations for the odd-odd In nuclei.

	106	108	110	112	114	116
$\tilde{\epsilon}_{1g_{9/2}}(\pi)$	0.00	0.00	0.00	0.00	0.00	0.00
$\tilde{\epsilon}_{2p_{1/2}}(\pi)$	0.95	0.90	0.90	0.80	0.70	0.60
$\tilde{\epsilon}_{2p_{3/2}}(\pi)$	1.80	1.70	1.60	1.40	1.30	1.30
$\tilde{\epsilon}_{1f_{7/2}}(\pi)$	2.40	2.30	2.20	2.10	2.05	2.00
$E_{1g_{7/2}}(\nu)$	0.00	0.00	0.00	0.00	0.24	0.54
$E_{2d_{5/2}}(\nu)$	0.00	0.40	0.58	0.69	1.09	1.34
$E_{3s_{1/2}}(\nu)$	0.50	0.43	0.33	0.15	0.00	0.00
$E_{2d_{3/2}}(\nu)$	1.08	0.91	0.72	0.45	0.25	0.15
$E_{1h_{11/2}}(\nu)$	1.92	1.63	1.21	0.75	0.46	0.25

normal ordering with respect to the neutron Bardeen-Cooper-Schrieffer (BCS) vacuum].

$$H_{\rm sh}(\pi)=\sum_{\pi}\tilde{\epsilon}(\pi)\tilde{a}_{\pi}\tilde{a}^{\dagger}_{\pi}$$

describes the unperturbed proton-hole energy [$\tilde{\epsilon}(\pi)$ denotes the proton-hole energy and $\tilde{a}_{\pi}$ the proton-hole creation operator]. $H_{\rm coupl}(\{^{\nu}_{\pi}\})$ describes the coupling between the neutron (proton) fermion degrees of freedom and the quadrupole vibrations. Finally $H_{\rm int}(\nu,\pi)$ describes the residual interaction between neutrons and protons. The explicit expression of $H_{\rm coupl}(\{^{\nu}_{\pi}\})$ is given by

$$H_{\rm coupl}(\{^{\nu}_{\pi}\})=-\sqrt{(\pi/5)}\xi_2(\{^{\nu}_{\pi}\})\hbar\omega_2\sum_{\{^{\nu\nu'}_{\pi\pi'}\}\mu}[b_{2\mu}+(-1)^{\mu}b^{\dagger}_{2-\mu}]\langle\{^{\nu'}_{\pi'}\}\,|\,Y_{2\mu}\,|\,\{^{\nu}_{\pi}\}\rangle\begin{Bmatrix}N(c^{\dagger}_{\nu}c_{\nu})\\ \tilde{a}_{\pi}\tilde{a}^{\dagger}_{\pi}\end{Bmatrix}. \tag{2.2}$$

To obtain energy spectra and wave functions, the Hamiltonian is diagonalized in the basis spanned by neutron-quasiparticle proton-hole multiplets coupled to the collective quadrupole excitations of the underlying core. Consequently the final wave functions can be expanded as

$$|JM;i\rangle=\sum d^{i}(NRI;J)\,|(N,R)\otimes[nlj(\nu)\otimes n'l'j'(\pi)]I;JM\rangle\ , \tag{2.3}$$

where N represents the number of quadrupole phonons (up to three quadrupole phonons were included in the calculation), R is the angular momentum of the quadrupole phonons, and $[nlj(\nu)\otimes n'l'j'(\pi)]$ I denotes the neutron-proton multiplet coupled to total angular momentum I. The neutron-proton model space consists of five subshells for the neutron-quasiparticle, i.e., $1g_{7/2}$, $2d_{5/2}$, $3s_{1/2}$, $2d_{3/2}$, and $1h_{11/2}$ and four subshells for the proton hole, i.e., $1g_{9/2}^{-1}$, $2p_{1/2}^{-1}$, $2p_{3/2}^{-1}$, and $1f_{5/2}^{-1}$.

B. Parameters

1. Neutron-quasiparticle energies

In order to obtain the neutron-quasiparticle energies and the occupation probabilities v^2, a BCS calculation was performed using the Nilsson Hamiltonian plus pairing force.[32] The values of μ and κ were taken from Ref. 33. The pairing strength $G(\nu)$ was adjusted in order to obtain the experimental odd-even mass difference. We refer to Tables I and II for further details. In Fig. 1 the neutron-quasiparticle energies are plotted as a function of neutron number. The lowest energies reproduce well the experimental trend of the ground states of the odd-mass Sn isotopes, i.e., in $^{107-111}$Sn this ground state is dominated by the $1g_{7/2}(\nu)$ orbit; for $A\geq 113$, the ground state has mainly a $3s_{1/2}(\nu)$ configuration.

2. Proton-hole energies

The values for the proton-hole energies are taken from particle-vibrational core coupling model calculations in

TABLE II. The Nilsson model parameters (μ,κ), the pairing strength G, and the pairing gap Δ for the odd-neutron system. The pairing strength G was adjusted to reproduce the experimental odd-even mass differences.

	106	108	110	112	114	116
$\mu(\nu)$	0.31	0.32	0.34	0.36	0.37	0.38
$\kappa(\nu)$	0.066	0.066	0.066	0.066	0.066	0.066
$G(\nu)$	0.1636	0.1606	0.1622	0.1549	0.1391	0.1410
$\Delta(\nu)$	1.050	1.250	1.305	1.277	1.008	1.191

TABLE III. The particle-core coupling strength $\xi_2(\nu)$, $\xi_2(\pi)$ [see Eq. (2.2)] and the phonon energy $\hbar\omega_2$ (in MeV) used in calculating the neutron-proton multiplets in odd-odd In nuclei.

	106	108	110	112	114	116
$\xi_2(\nu)$	3.75	3.50	3.25	3.00	2.75	2.50
$\xi_2(\pi)$	2.75	2.50	2.25	2.00	1.75	1.50
$\hbar\omega_2$	1.200	1.210	1.215	1.250	1.300	1.230

the odd-mass In isotopes.[11-13] The parameters are given in Table I.

3. *Particle-core coupling strengths*

These parameters determine the splitting of the neutron-proton multiplet. It was pointed out that the energy splitting of the ν-π multiplet is roughly a parabola as a function of $I(I+I)$.[34] The spin I_l of the lowest member of the multiplet is given by

$$I_l \simeq [j_\nu(j_\nu+1)+j_\pi(j_\pi+1)-\tfrac{1}{4}]^{1/2}-\tfrac{1}{2} . \tag{2.4}$$

When applying the parabolic rule (2.4) (as discussed extensively by Paar[34]) to the $1h_{11/2}(\nu)$-$1g_{9/2}^{-1}(\pi)$ multiplet, the spin of the negative parity band head should be 7. This is verified in the case of $^{106-110}$In. The disagreement for the $^{112-116}$In isotopes can be understood when considering the neutron-proton interaction. We come to this point later in this paper.

As a first estimate for the particle-core coupling strengths, the values from the particle-core calculations in odd-mass In isotopes were taken.[11-13] However, a better agreement with experiment is obtained by varying these values somewhat. The results are given in Table III.

4. *The neutron-proton interaction*

The residual neutron-proton interaction was assumed to be

$$H_{\rm int}(\nu,\pi)=[(1-\alpha)+\alpha\boldsymbol{\sigma}_\nu\cdot\boldsymbol{\sigma}_\pi]\sum_{\lambda=2,4}\chi_\lambda Q_\lambda(\nu)\cdot Q_\lambda(\pi) , \tag{2.5}$$

where

$$Q_{\lambda\mu}(i)\equiv r_i^\lambda Y_{\lambda\mu}(\theta_i,\phi_i) \quad (i=\nu,\pi) . \tag{2.6}$$

As already mentioned above, the neutron-proton interaction also plays a role in the splitting of a neutron-proton multiplet. For a $Q_2(\nu)\cdot Q_2(\pi)$ interaction without spin dependence, the energy splitting of a ν-π multiplet is a parabola as a function of $I(I+1)$. In Fig. 2, this is illustrated in the case of the $1h_{11/2}(\nu)$-$1g_{9/2}^{-1}(\pi)$ multiplet. In that case such an interaction would give the 7^- as the band head of the corresponding negative parity band. In the same figure the energy splitting of a spin-independent $Q_4(\nu)\cdot Q_4(\pi)$ interaction is drawn. When adding up the $Q_2(\nu)\cdot Q_2(\pi)$ and the $Q_4(\nu)\cdot Q_4(\pi)$ contribution, the 8^- state becomes below the 7^- state. In the present calculation, we used $\chi_2=-0.175$ MeV and $\chi_4=-0.005$ MeV, yielding the best agreement with the experimentally observed band states. We can thus conclude the following: Whereas the particle-core interaction tends to position the 7^- below the 8^- state, the ν-π interaction with both $\lambda=2$ and 4 multipoles favors the 8^- to be the lowest level. The spin dependence almost does not change this conclusion.

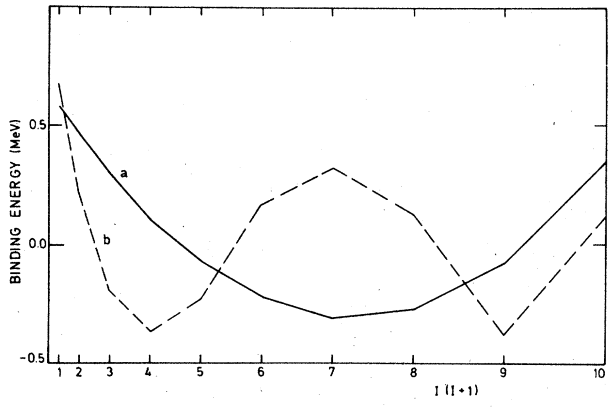

FIG. 2. (a) Splitting of the $[1h_{11/2}(\nu)$-$1g_{9/2}^{-1}(\pi)]$ multiplet due to the $\chi_2 Q_2(\nu)\cdot Q_2(\pi)$ interaction as a function of $I(I+1)$ ($\chi_2=-0.175$ MeV). (b) Splitting of the same multiplet due to the $\chi_4 Q_4(\nu)\cdot Q_4(\pi)$ interaction as a function of $I(I+1)$ ($\chi_4=-0.005$ MeV).

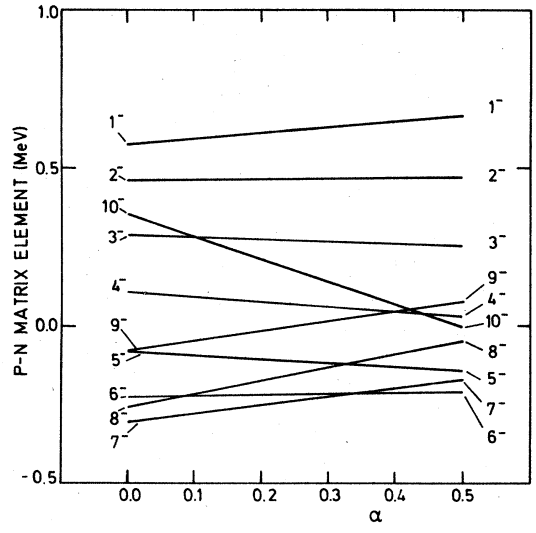

FIG. 3. The neutron-proton matrix elements

$$\langle 1h_{11/2}(\nu)\otimes 1g_{9/2}^{-1}(\pi);I \,|\, [(1-\alpha)+\alpha\boldsymbol{\sigma}_\nu\cdot\boldsymbol{\sigma}_\pi]\chi_2 Q_2(\nu)\cdot Q_2(\pi) \,|\, 1h_{11/2}(\nu)\otimes 1g_{9/2}^{-1}(\pi);I\rangle ,$$

as a function of α using $\chi_2=-0.175$ MeV.

We refer to Fig. 3 for the influence of α on the negative parity multiplet. The value of $\alpha=0.25$ was fitted in order to get the best agreement with the experimentally observed negative parity band. Moreover a spin-independent interaction would not reproduce the 1^+ as the ground state of $^{112-116}$In. In Sec. III we will discuss the combined effect of the particle-core coupling and the neutron-proton interaction on the $1h_{11/2}(\nu)$-$1g_{9/2}^{-1}(\pi)$ multiplet.

III. APPLICATION TO ODD-ODD IN NUCLEI

A. Energy and wave functions

In Fig. 4 the experimental and theoretical results for $^{106-116}$In are shown. The general trends are well reproduced:

(i) The lowering of the negative parity band can be un-

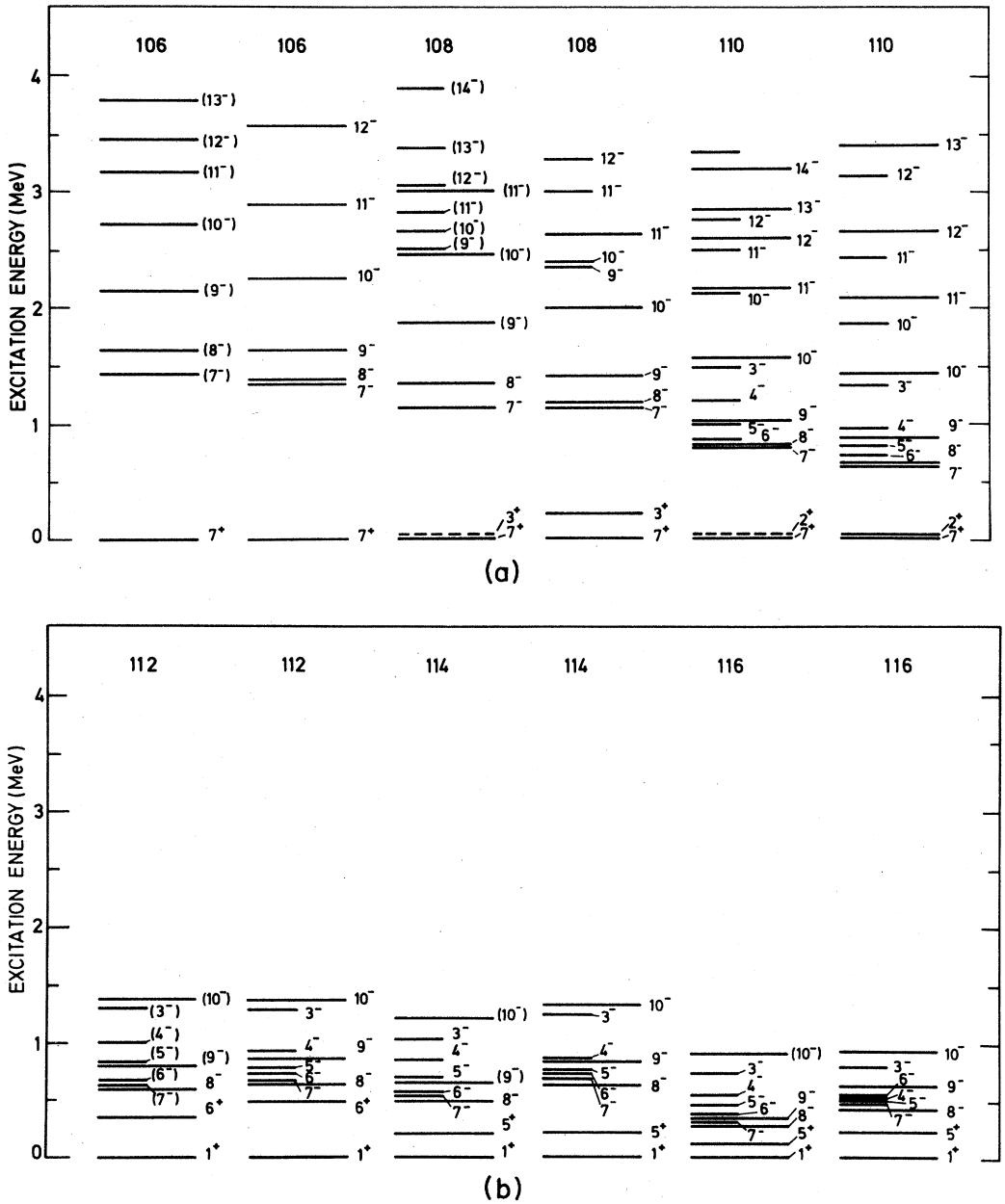

FIG. 4. (a) Experimental and theoretical neutron-proton multiplets in the odd-odd $^{106-110}$In nuclei. The members of a possible second high-spin multiplet and the low-spin members of the $[1h_{11/2}(\nu)$-$1g_{9/2}^{-1}(\pi)]I$ multiplet, i.e., 3^-, 4^-, 5^-,6^-, and 7^-, are drawn with a short line. Positive parity states for which static moments are known, i.e., 7^+, 2^+, and 3^+ (see also Table VI), are also drawn. In ^{108,110}In, the experimental isomeric 3^+ and 2^+ levels, respectively, are drawn with a dashed line (excitation energy relative to the 7^+ level unknown). (b) Same caption as for (a) but for $^{112-116}$In. Positive parity states for which static moments are known, i.e., 1^+, 5^+, 6^+, are also drawn (see also Table VI).

TABLE IV. The main components for the low-lying neutron-proton multiplet states in ^{112}In. The notation used is $|(N,R)\otimes[nlj(\nu)\otimes n'l'j'(\pi)]I;J^{\pi}\rangle$.

$$
\begin{aligned}
|1^+\rangle &= +0.85\,|(0,0)\otimes[1g_{7/2}(\nu)\otimes 1g_{9/2}(\pi)]1;1^+\rangle \\
&\quad -0.33\,|(1,2)\otimes[1g_{7/2}(\nu)\otimes 1g_{9/2}(\pi)]2;1^+\rangle \\
&\quad +0.24\,|(1,2)\otimes[1g_{7/2}(\nu)\otimes 1g_{9/2}(\pi)]3;1^+\rangle \\
|6^+\rangle &= -0.63\,|(0,0)\otimes[1g_{7/2}(\nu)\otimes 1g_{9/2}(\pi)]6;6^+\rangle \\
&\quad -0.36\,|(1,2)\otimes[1g_{7/2}(\nu)\otimes 1g_{9/2}(\pi)]6;6^+\rangle \\
&\quad -0.30\,|(1,2)\otimes[2d_{3/2}(\nu)\otimes 1g_{9/2}(\pi)]5;6^+\rangle \\
|8^-\rangle &= -0.73\,|(0,0)\otimes[1h_{11/2}(\nu)\otimes 1g_{9/2}(\pi)]8;8^-\rangle \\
&\quad +0.42\,|(1,2)\otimes[1h_{11/2}(\nu)\otimes 1g_{9/2}(\pi)]7;8^-\rangle \\
&\quad -0.40\,|(1,2)\otimes[1h_{11/2}(\nu)\otimes 1g_{9/2}(\pi)]9;8^-\rangle \\
|7^-\rangle &= -0.68\,|(0,0)\otimes[1h_{11/2}(\nu)\otimes 1g_{9/2}(\pi)]7;7^-\rangle \\
&\quad +0.47\,|(1,2)\otimes[1h_{11/2}(\nu)\otimes 1g_{9/2}(\pi)]8;7^-\rangle \\
&\quad -0.39\,|(1,2)\otimes[1h_{11/2}(\nu)\otimes 1g_{9/2}(\pi)]6;7^-\rangle \\
|9^-\rangle &= +0.74\,|(0,0)\otimes[1h_{11/2}(\nu)\otimes 1g_{9/2}(\pi)]9;9^-\rangle \\
&\quad +0.50\,|(1,2)\otimes[1h_{11/2}(\nu)\otimes 1g_{9/2}(\pi)]8;9^-\rangle \\
&\quad -0.27\,|(1,2)\otimes[1h_{11/2}(\nu)\otimes 1g_{9/2}(\pi)]10;9^-\rangle \\
|10^-\rangle &= +0.71\,|(0,0)\otimes[1h_{11/2}(\nu)\otimes 1g_{9/2}(\pi)]10;10^-\rangle \\
&\quad +0.59\,|(1,2)\otimes[1h_{11/2}(\nu)\otimes 1g_{9/2}(\pi)]9;10^-\rangle \\
&\quad +0.23\,|(2,4)\otimes[1h_{11/2}(\nu)\otimes 1g_{9/2}(\pi)]8;10^-\rangle \\
|6^-\rangle &= -0.70\,|(0,0)\otimes[1h_{11/2}(\nu)\otimes 1g_{9/2}(\pi)]6;6^-\rangle \\
&\quad +0.46\,|(1,2)\otimes[1h_{11/2}(\nu)\otimes 1g_{9/2}(\pi)]7;6^-\rangle \\
&\quad -0.38\,|(1,2)\otimes[1h_{11/2}(\nu)\otimes 1g_{9/2}(\pi)]8;6^-\rangle \\
|5^-\rangle &= -0.76\,|(0,0)\otimes[1h_{11/2}(\nu)\otimes 1g_{9/2}(\pi)]5;5^-\rangle \\
&\quad +0.44\,|(0,0)\otimes[1h_{11/2}(\nu)\otimes 1g_{9/2}(\pi)]6;5^-\rangle \\
&\quad -0.33\,|(0,0)\otimes[1h_{11/2}(\nu)\otimes 1g_{9/2}(\pi)]4;5^-\rangle \\
|4^-\rangle &= -0.81\,|(0,0)\otimes[1h_{11/2}(\nu)\otimes 1g_{9/2}(\pi)]4;4^-\rangle \\
&\quad +0.44\,|(1,2)\otimes[1h_{11/2}(\nu)\otimes 1g_{9/2}(\pi)]5;4^-\rangle \\
&\quad -0.23\,|(1,2)\otimes[1h_{11/2}(\nu)\otimes 1g_{9/2}(\pi)]3;4^-\rangle \\
|3^-\rangle &= -0.81\,|(0,0)\otimes[1h_{11/2}(\nu)\otimes 1g_{9/2}(\pi)]3;3^-\rangle \\
&\quad +0.47\,|(1,2)\otimes[1h_{11/2}(\nu)\otimes 1g_{9/2}(\pi)]4;3^-\rangle \\
&\quad -0.13\,|(1,2)\otimes[1h_{11/2}(\nu)\otimes 1g_{9/2}(\pi)]2;3^-\rangle
\end{aligned}
$$

derstood when examining the main components of the wave functions (See Table IV for the case of ^{112}In). One can see that the members of the negative parity band are almost pure $1h_{11/2}(\nu)$-$1g_{9/2}^{-1}(\pi)$ configurations coupled to the vibrational core excitations. In first order, the energy

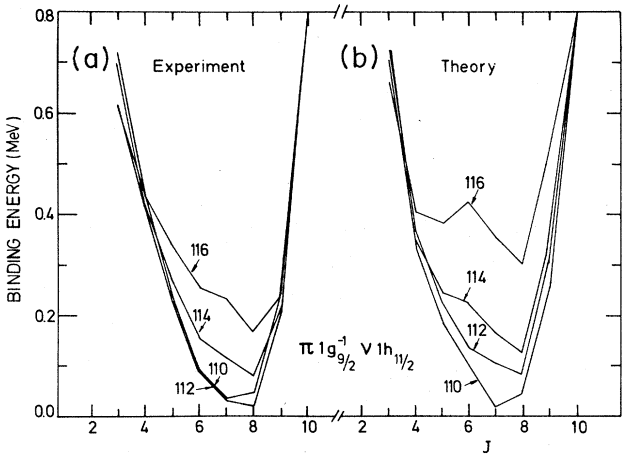

FIG. 5. (a) Experimental splitting of the $[1h_{11/2}(\nu)$-$1g_{9/2}^{-1}(\pi)]I$ multiplet relative to the 10^- level as a function of I. (b) Same caption as for (a) but for the theoretical multiplet.

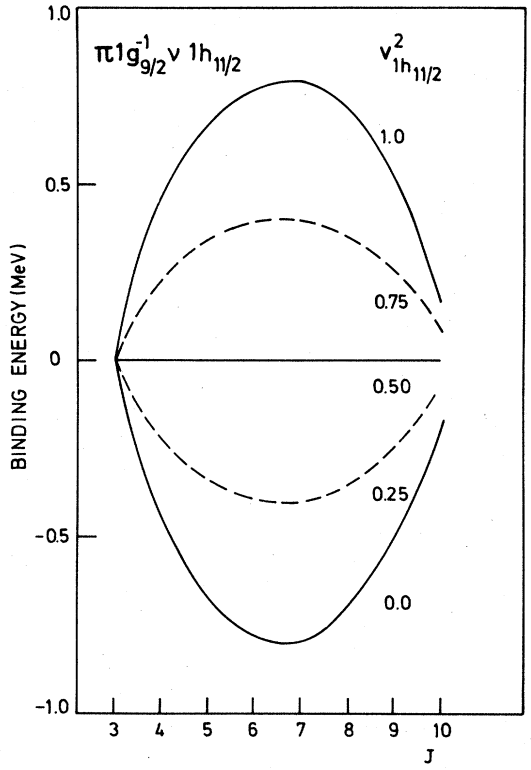

FIG. 6. Schematic illustration of the splitting of the $[1h_{11/2}(\nu)$-$1g_{9/2}^{-1}(\pi)]$ multiplet as a function of I, for different values of $v^2_{1h_{11/2}}$.

position of the band is determined by

$$E_{1h_{11/2}}(\nu)+\tilde{\epsilon}_{1g_{9/2}}(\pi)\simeq E_{1h_{11/2}}(\nu)\ .$$

In Fig. 1, one can clearly see how the energy of the $1h_{11/2}(\nu)$ orbit decreases as the mass number increases.

(ii) The negative parity band becomes more compressed as the neutron number increases. The particular levels mainly originating from the $1h_{11/2}(\nu)$-$1g_{9/2}^{-1}(\pi)$ configuration are shown in Fig. 5(a) where, relative to the 10^- level and for $^{110-116}$In, the different members are shown. In Fig. 5(b), the analogous theoretical multiplet members are shown. The overall good agreement is striking: it is due to the strength of the neutron-proton interaction and particle-core interaction, and the subsequent filling of the neutron $1h_{11/2}$ orbital. If, in a first approximation, the neutron-core and proton-core strengths are taken equal to each other and in addition the spin dependence of the neutron-proton force is neglected, it is easily proven that the matrix elements responsible for the splitting of the multiplet are proportional to the pairing factor

$$[u^2_{1h_{11/2}}(\nu)-v^2_{1h_{11/2}}(\nu)]\ .$$

As can be read from Table V,

$$[u^2_{1h_{11/2}}(\nu)-v^2_{1h_{11/2}}(\nu)]$$

becomes smaller with increasing neutron number. This is illustrated by considering the diagonal ν-π two-body matrix elements for the pure proton-hole neutron quasiparticle

TABLE V. The occupation probabilities $v^2(\nu)$ and the differences $[u^2(\nu)-v^2(\nu)]$, as calculated from the Nilsson model, including pairing.

		106	108	110	112	114	116
v^2	$1h_{11/2}(\nu)$	0.027	0.045	0.073	0.102	0.118	0.207
	$1g_{7/2}(\nu)$	0.203	0.359	0.521	0.674	0.832	0.869
	$2d_{5/2}(\nu)$	0.797	0.845	0.860	0.892	0.943	0.944
	$2d_{3/2}(\nu)$	0.051	0.082	0.118	0.145	0.164	0.253
	$3s_{1/2}(\nu)$	0.092	0.149	0.198	0.234	0.289	0.399
u^2-v^2	$1h_{11/2}(\nu)$	0.946	0.910	0.854	0.796	0.764	0.586
	$1g_{7/2}(\nu)$	0.593	0.282	−0.042	−0.348	−0.664	−0.738
	$2d_{5/2}(\nu)$	−0.594	−0.690	−0.720	−0.784	−0.880	−0.880
	$2d_{3/2}(\nu)$	0.897	0.836	0.764	0.710	0.672	0.494
	$3s_{1/2}(\nu)$	0.814	0.702	0.604	0.532	0.422	0.202

$$\langle 1h_{11/2}(\nu)\otimes 1g_{9/2}^{-1}(\pi);I \mid H_{\rm int}(\nu,\pi) \mid 1h_{11/2}(\nu)\otimes 1g_{9/2}^{-1}(\pi);I\rangle_{\rm qp}$$
$$= v^2_{1h_{11/2}}\langle 1h_{11/2}(\nu)\otimes 1g_{9/2}(\pi);I \mid H_{\rm int}(\nu,\pi) \mid 1h_{11/2}(\nu)\otimes 1g_{9/2}(\pi);I\rangle_{\rm pp}$$
$$+ u^2_{1h_{11/2}}\langle 1h_{11/2}(\nu)\otimes 1g_{9/2}^{-1}(\pi);I \mid H_{\rm int}(\nu,\pi) \mid 1h_{11/2}(\nu)\otimes 1g_{9/2}^{-1}(\pi);I\rangle_{\rm ph} . \quad (3.1)$$

This expression (3.1) clearly explains the gradual change from a particle-hole spectrum (as is the case in ^{110,112}In) towards a hole-hole spectrum (for the heavy odd-odd In nuclei). One can thus expect that near mass $A\simeq 120$, 122 all multiplet members should be almost degenerate in energy, due to a cancellation between the attractive particle-hole and repulsive hole-hole matrix elements (relative to the 10^- configuration). The corresponding change in the energy splitting of the multiplet is schematically illustrated in Fig. 6 for a gradual filling of the $1h_{11/2}$ neutron orbital.

The position of the 7^- level with respect to the 8^- level is reversed for $A \geq 112$. This is an effect of the competition between the neutron-proton interaction and the particle-core strength. For $A < 112$, the order of the 7^- and the 8^- levels is dominated by the particle-core interaction which tends to keep the 7^- below the 8^-. For $A \geq 112$, the neutron-proton interaction which tends to

TABLE VI. Magnetic dipole moments and electric quadrupole moments (in units μ_N and $e\,b$, respectively) for $^{106-116}$In low-lying levels.

		Magnetic moments (μ_N)		Quadrupole moments ($e\,b$)	
	J^π	Experiment	Theory	Experiment	Theory
^{106}In	7^+	4.925(13)[a]	4.415		
^{108}In	7^+	4.53(10)[b]	5.40		
	3^+	3.10(30)[b]	3.71		
^{110}In	2^+	4.365(4)[c]	4.175	0.37[c]	0.24
	7^+	4.719(13)[d]	4.876	−0.215[c]	0.60
				+0.230[c]	
^{112}In	1^+	2.82(3)[c]	2.84	0.093[c]	0.102
	6^+	4.056(36)[e]	5.396	0.75(15)[j]	0.34
	8^-	3.080(32)[e]	3.232	0.093(6)[k]	−0.043
^{114}In	1^+	2.815(11)[f]	2.837		
	5^+	4.658(14)[g]	5.028		
^{116}In	1^+	2.7867(8)[h]	2.842		
		2.7889(10)[i]			
	5^+	4.22(8)[c]	4.92		
		4.4(1)[c]			

[a]The experimental data are from Ref. 19.
[b]The experimental data are from Ref. 20.
[c]The experimental data are from Ref. 21.
[d]The experimental data are from Ref. 22.
[e]The experimental data are from Ref. 23.
[f]The experimental data are from Ref. 24.
[g]The experimental data are from Ref. 25.
[h]The experimental data are from Ref. 26.
[i]The experimental data are from Ref. 27
[j]The experimental data are from Ref. 28.
[k]The experimental data are from Ref. 29.

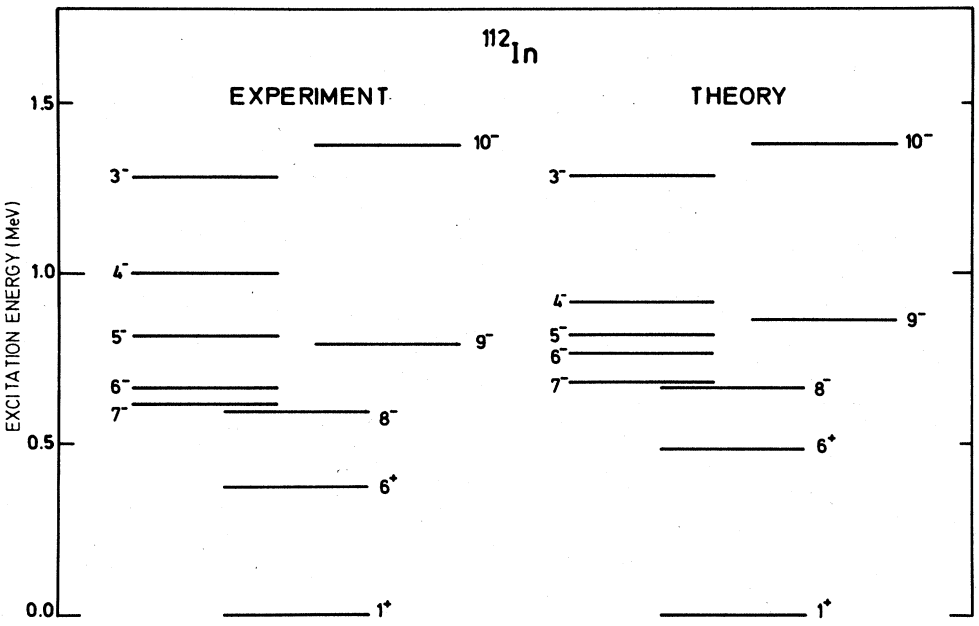

FIG. 7. The theoretical and experimental (Refs. 2 and 6) low-lying levels in ^{112}In. The high-spin members $(9^-,10^-)$ are drawn well separated from the low-spin states $(3^-,\ldots,7^-)$ in order to make the figure more transparent. The ground state 1^+ and the 6^+ level are also drawn (levels for which static moments have been measured, see also Table VI).

have the 8^- below the 7^-, changes the level sequence.

Concerning the wave functions, we consider the example of ^{112}In. From Fig. 7 we observe that the experimental energy levels are well reproduced. Table IV shows the main components of the corresponding wave functions.

(i) The 1^+ ground state is almost purely based on the $1g_{7/2}(\nu)$-$1g_{9/2}^{-1}(\pi)$ multiplet whereas the 6^+ state contains admixtures of the $2d_{5/2}(\nu)$-$1g_{9/2}^{-1}(\pi)$ multiplet. When applying the parabolic rule[34] to the ground state multiplet, the ground state spin should be given by

$$I=\{\tfrac{7}{2}\cdot\tfrac{9}{2}+\tfrac{9}{2}\cdot\tfrac{11}{2}-\tfrac{1}{4}\}^{1/2}-\tfrac{1}{2}=6\ .$$

This deviation from experiment can be explained by the fact that correlations other than the collective quadrupole mode are important: spin-dependent $\lambda=2$ and 4 neutron-proton interactions and configuration mixing.

(ii) The members of the negative parity band contain pure $1h_{11/2}(\nu)$-$1g_{9/2}^{-1}(\pi)$ excitations. As already explained in Sec. II, we can attribute the deviation from the parabolic rule[34] for the ground state of this multiplet to the specific neutron-proton interaction. It is also noted that the higher the excitation energy of the band member, the more important the higher-phonon contributions become (See also Ref. 18). The members of the negative-parity band are mainly based upon the zero- and one-phonon components, whereas the members of a possible second band (levels drawn with a short line in Fig. 4) mainly contain one- and two-phonon admixtures [coupled to the $1h_{11/2}(\nu)$-$1g_{9/2}^{-1}(\pi)$ multiplet].

B. Magnetic and quadrupole moments

A test on the wave functions is provided by the calculation of magnetic and quadrupole moments. As effective spin gyromagnetic factors, half the free proton and neutron values are used, i.e., $g_s(\nu)=+2.7928\mu_N$ and $g_s(\pi)=-1.913\,15\mu_N$, $g_l(\nu)$ and $g_l(\pi)$ were taken equal to $0\mu_N$ and $1\mu_N$, respectively. The collective gyromagnetic factor can be approximated by $g_R=Z/A$. When calcu-

TABLE VII. See caption of Table IV, but now for the 7^+, 1^+, 5^+, 3^+, and 2^+ levels in $^{106-116}$In.

^{106}In	$\|7^+\rangle=-0.66\,\|(1,2)\otimes[2d_{5/2}(\nu)\otimes 1g_{9/2}(\pi)]7;7^+\rangle$
	$+0.61\,\|(0,0)\otimes[2d_{5/2}(\nu)\otimes 1g_{9/2}(\pi)]7;7^+\rangle$
^{108}In	$\|7^+\rangle=-0.63\,\|(0,0)\otimes[1g_{7/2}(\nu)\otimes 1g_{9/2}(\pi)]7;7^+\rangle$
	$-0.37\,\|(1,2)\otimes[1g_{7/2}(\nu)\otimes 1g_{9/2}(\pi)]7;7^+\rangle$
	$\|3^+\rangle=+0.62\,\|(0,0)\otimes[1g_{7/2}(\nu)\otimes 1g_{9/2}(\pi)]3;3^+\rangle$
	$-0.34\,\|(1,2)\otimes[1g_{7/2}(\nu)\otimes 1g_{9/2}(\pi)]4;3^+\rangle$
^{110}In	$\|2^+\rangle=-0.59\,\|(0,0)\otimes[2d_{5/2}(\nu)\otimes 1g_{9/2}(\pi)]2;2^+\rangle$
	$-0.44\,\|(0,0)\otimes[1g_{7/2}(\nu)\otimes 1g_{9/2}(\pi)]2;2^+\rangle$
	$+0.34\,\|(1,2)\otimes[2d_{5/2}(\nu)\otimes 1g_{9/2}(\pi)]3;2^+\rangle$
	$\|7^+\rangle=-0.59\,\|(0,0)\otimes[1g_{7/2}(\nu)\otimes 1g_{9/2}(\pi)]7;7^+\rangle$
	$-0.40\,\|(0,0)\otimes[2d_{5/2}(\nu)\otimes 1g_{9/2}(\pi)]7;7^+\rangle$
	$+0.38\,\|(1,2)\otimes[2d_{5/2}(\nu)\otimes 1g_{9/2}(\pi)]7;7^+\rangle$
	$-0.31\,\|(1,2)\otimes[1g_{7/2}(\nu)\otimes 1g_{9/2}(\pi)]7;7^+\rangle$
^{114}In	$\|1^+\rangle=+0.83\,\|(0,0)\otimes[1g_{7/2}(\nu)\otimes 1g_{9/2}(\pi)]1;1^+\rangle$
	$-0.34\,\|(1,2)\otimes[1g_{7/2}(\nu)\otimes 1g_{9/2}(\pi)]2;1^+\rangle$
	$\|5^+\rangle=-0.60\,\|(0,0)\otimes[3s_{1/2}(\nu)\otimes 1g_{9/2}(\pi)]5;5^+\rangle$
	$-0.40\,\|(1,2)\otimes[3s_{1/2}(\nu)\otimes 1g_{9/2}(\pi)]5;5^+\rangle$
	$-0.38\,\|(0,0)\otimes[2d_{3/2}(\nu)\otimes 1g_{9/2}(\pi)]5;5^+\rangle$
^{116}In	$\|1^+\rangle=+0.85\,\|(0,0)\otimes[1g_{7/2}(\nu)\otimes 1g_{9/2}(\pi)]1;1^+\rangle$
	$-0.32\,\|(1,2)\otimes[1g_{7/2}(\nu)\otimes 1g_{9/2}(\pi)]2;1^+\rangle$
	$\|5^+\rangle=-0.59\,\|(0,0)\otimes[2d_{3/2}(\nu)\otimes 1g_{9/2}(\pi)]5;5^+\rangle$
	$-0.57\,\|(0,0)\otimes[3s_{1/2}(\nu)\otimes 1g_{9/2}(\pi)]5;5^+\rangle$
	$-0.32\,\|(1,2)\otimes[2d_{3/2}(\nu)\otimes 1g_{9/2}(\pi)]5;5^+\rangle$

lating the quadrupole moments, the following effective charges were used: $e_\nu = 0.5e$, $e_\pi = 1.5e$, $e_{\text{vibr}} = 1.3e$.

In Table VI, we compare the experimental values with the theoretical results. In general, the correct order of magnitude is obtained. The details of the calculation show that in all cases the contributions of the collective operator to the total magnetic moment is negligible. For the 1^+ states the major contribution comes from the main component of the wave function, i.e., the $1g_{7/2}(\nu)$-$1g_{9/2}^{-1}(\pi)$ multiplet. The increasing trend for the magnetic moment of the 5^+ state in going from ^{114}In to ^{116}In is reproduced. However, the decreasing and increasing trend for the magnetic moment of the 7^+ state in going from ^{106}In to ^{108}In and from ^{108}In to ^{110}In, respectively, is not reproduced. In Table VII, we see the different structure of the 7^+ state for the three isotopes. The 7^+ state in ^{106}In is mainly based on the $2d_{5/2}(\nu)$-$1g_{9/2}^{-1}(\pi)$ multiplet, whereas in ^{108}In it is built upon the $1g_{7/2}(\nu)$-$1g_{9/2}^{-1}(\pi)$ multiplet. In ^{110}In, the 7^+ state is an admixture of the two multiplets just mentioned. As to the quadrupole moments, detailed calculations indicate an important contribution of about 50% (and even more in the case of the 8^- state in ^{112}In) due to the collective operator. This explains why models containing no collectivity (Refs. 4 and 5) give a quadrupole moment which is about 50% too small. The negative sign for the quadrupole moment of the 8^- state in ^{112}In is largely due to the contribution of the collective operator. We refer to Table VII for the wave functions of the states discussed in this section.

IV. CONCLUSION

In the framework of the neutron-quasiparticle proton-hole quadrupole core coupling model, we were able to understand the general features of the observed collective negative parity bands through a range of odd-odd In isotopes. Within the same model, we compared theoretical magnetic and quadrupole moments of ground and isomeric states with the experimental values.

We finally stress the fact that the negative parity band has an almost pure multiplet configuration. This means, from a theoretical point of view, that our understanding and conclusions are not obscured by multiplet configuration mixing. Therefore both further experimental and theoretical investigation for such pure cases in odd-odd nuclei should deserve our attention.

ACKNOWLEDGMENTS

The authors are grateful to V. Paar for discussions on the relevance of studying odd-odd nuclei. Two of the authors (J.V.M. and K.H.) are grateful to the Institut de Physique Nucléaire (IPN) and IN2P3 (Lyon) for financial support in various stages of this work.

*Present address: SIDEL, PC-Division, Gouvernementstraat 32,B-9000 Gent, Belgium.

†Also at: Rijksuniversiteit Gent, STVS&LEKF, Krijgslaan 281,S9,B-9000.

[1]D. Rabenstein, D. Harrach, H. Vonach, G. G. Dussel, and R. P. I. Perazzo, Nucl. Phys. **A197**, 129 (1972).

[2]M. Eibert, A. K. Gaigalas, and N. I. Greeberg, J. Phys. G **2**, L203 (1976).

[3]V. L. Alexeev, B. A. Emelianov, D. M. Kaminiker, Yu. L. Khazov, I. A. Kondurov, Yu. E. Loginov, V. L. Rumiantsev, S. L. Sakharov, and A. I. Smirov, Nucl. Phys. **A262**, 19 (1976).

[4]W. F. Van Gunsteren, Nucl. Phys. **A265**, 263 (1976).

[5]W. F. Van Gunsteren, K. Allaart, and E. Boeker, Nucl. Phys. **A266**, 365 (1976).

[6]T. Kohno, M. Adachi, and H. Taketani, Nucl. Phys. **A398**, 493 (1983).

[7]N. Elias, R. Béraud, A. Charvet, R. Duffait, R. Meyer, S. André, J. Genevey, S. Tedesco, and J. Tréherne, Nucl. Phys. **A351**, 142 (1981).

[8]R. Béraud, A. Charvet, R. Duffait, M. Meyer, J. Genevey, J. Tréherne, A. Genoux-Lubain, F. Beck, and T. Bryrski, J. Phys. (Paris) **C10**, 159 (1980).

[9]B. Roussière, P. Kilcher, J. Sauvage-Letessier, C. Bourgeois, the ISOCELE collaboration, R. Béraud, R. Duffait, M. Meyer, J. Genevey-Rivier, and J. Tréherne, Nucl. Phys. **A419**, 61 (1984).

[10]I. N. Wischnewski, H. V. Klapdor, H. Fromm, and P. Herges, Z. Phys. A **300**, 300 (1981).

[11]K. Heyde, M. Waroquier, and A. Meyer, Phys. Rev. C **17**, 1219 (1978).

[12]M. D. Glascock, E. W. Schneider, W. B. Walters, S. V. Jackson, and R. A. Meyer, Phys. Rev. C **20**, 2370 (1979).

[13]K. Heyde, M. Warouier, and P. Van Isacker, Phys. Rev. C **22**, 1267 (1980).

[14]W. H. A. Hesselink, J. Bron, P. M. A. Van der Kam, V. Paar, A. Van Poelgeest, and A. G. Zephat, Nucl. Phys. **A299**, 60 (1978).

[15]J. Bron, J. J. A. Zalmstra, M. J. Uitzinger, H. Verheul, S. J. Feenstra, and J. Van Klinken, Nucl. Phys. **A327**, 12 (1979).

[16]P. Van Nes *et al.*, Nucl. Phys. **A379**, 35 (1982).

[17]R. Duffait, J. Van Maldeghem, A. Charvet, J. Sau, K. Heyde, A. Emsallem, M. Meyer, R. Béraud, J. Tréherne, and J. Genevey, Z. Phys. A **307**, 259 (1982).

[18]J. Van Maldeghem, J. Sau, and K. Heyde, Phys. Lett. **116B**, 387 (1982).

[19]D. Vandeplassche, E. Van Walle, and D. Wouters (private communication).

[20]D. Vandeplassche, E. Van Walle, C. Nuytten, and L. Vanneste, Nucl. Phys. **A396**, 115c (1983).

[21]*Table of Nuclear Moments,* edited by V. S. Shirley and C. M. Lederer (Wiley, New York, 1978).

[22]E. Hagn and E. Zech, Z. Phys. A **300**, 339 (1981).

[23]M. Ionesco-Bujor, E. A. Ivanov, A. Iordachescu, P. Plostinaru, and G. Pascovici, Nucl. Phys. **A272**, 1 (1976).

[24]C. Nuytten, D. Vandenplassche, E. Van Walle, and L. Vanneste, Phys. Rev. C **26**, 1701 (1982).

[25]W. W. Lattimer and N. J. Stone, Hyp. Int. **7**, 61 (1979).

[26]H. Lades, Z. Phys. **252**, 242 (1972).

[27]A. Winnacker, H. Ackermann, D. Dubbers, and J. Mertens, Z. Phys. **244**, 289 (1971).

[28]M. Ionescu-Bujor, A. Iordachescu, E. A. Ivanov, and D. Plostinaru, Hyp. Int. **11**, 71 (1981).

[29]M. Ionescu-Bujor, E. A. Ivanov, A. Iordachescu, D. Plos-

tinaru, and G. Pascovici, Phys. Lett. **64B**, 36 (1976).
[30]D. Vandeplassche, E. Van Walle, C. Nuytten, and L. Vanneste, Phys. Rev. Lett. **49**, 1390 (1982).
[31]B. W. Filippone, C. N. Davids, R. C. Pardo, and J. Äystö, Phys. Rev. C **29**, 2118 (1984).
[32]P. Ring and P. Schuck, *The Nuclear Many-Body Problem* (Springer, Berlin, 1980).
[33]J. Moreau, Lic. thesis, Rijksuniversiteit, 1980.
[34]V. Paar, Nucl. Phys. **A331**, 16 (1979).